Monthly Notices
of the
ROYAL ASTRONOMICAL SOCIETY

MNRAS **430,** 2154–2168 (2013) doi:10.1093/mnras/stt036

Study of photospheric, chromospheric and coronal activities of V1147 Tau

Manoj K. Patel,[1]⋆ J. C. Pandey,[2] Igor S. Savanov,[3] Vinod Prasad[1] and D. C. Srivastava[1]

[1]*Department of Physics, D. D. U. Gorakhpur University, Gorakhpur 273009, India*
[2]*Aryabhatta Research Institute of Observational Sciences (ARIES), Nainital 263129, India*
[3]*Institute of Astronomy, Russian Academy of Sciences, ul. Pyatnitskaya 48, Moscow 119017, Russia*

Accepted 2013 January 7. Received 2013 January 2; in original form 2012 April 13

ABSTRACT

We present analyses of optical photometric, spectroscopic, polarimetric and X-ray observations of the K5V binary star, V1147 Tau. Nearly 20 yr of optical observations show that V1147 Tau is a periodic variable with a photometric period of 1.4845 ± 0.0001 d. Light curves observed at 16 epochs show changes in minima, amplitude and shape indicating that the variability is due to the presence of surface inhomogeneities. The surface coverage of spots was found to be in the range of 9–22 per cent. Most of the time, the spots were resolved as two active longitudes. Switching of dominant active longitudes was also seen. The optical spectroscopy revealed that Hα is present in emission, indicating a high level of chromospheric activity. The polarimetric observations yield average values of polarization to be 0.40 ± 0.03, 0.22 ± 0.05, 0.17 ± 0.07 and 0.12 ± 0.04 per cent in *B, V, R* and *I* bands, respectively, which indicates the possibility of scattering by thin circumstellar material. The X-ray light curve was found to be rotationally modulated and was anticorrelated with optical light curves observed at quasi-simultaneous epochs. The corona of V1147 Tau consists of a two temperature plasma with $kT_1 = 0.07$ keV and $kT_2 = 0.66$ keV. The X-ray luminosity in the 0.2–2.4 keV energy band was found to be $4.4–6.8 \times 10^{29}$ erg s^{-1}. Flaring features were also seen in the X-ray light curve.

Key words: polarization – stars: activity – stars: coronae – stars: individual: V1147 Tau – stars: magnetic field – starspots.

1 INTRODUCTION

Stars cooler than F-type show activity phenomena that appear analogous to the features observed on the Sun. These features are expected on the basis of the dynamo theory of magnetic field generation as the stars have a radiative core and convective outer envelope with an interface where strong shear leads to amplification of magnetic fields (Durney & Robinson 1982; Baliunas et al. 1983; Gilman 1983; Mohanty & Basri 2003; Dobler et al. 2006). Further, these stars have inhomogeneities on their surfaces that may cause variation in their light curves and many spectral lines in the optical and infrared (IR) bands. The periodic light variations observed in such types of stars are of the order of few millimagnitudes to a fraction of a magnitude with periods ranging from a few hours to several days. The magnetic fields reach into the corona and into the stellar environment, structuring it and governing heating and particle acceleration. This phenomenon is responsible for the ultraviolet (UV), X-ray and radio emission in these stars. Magnetic phenomena dominate the activity of all stars with convective outer envelopes, from young T Tauri stars, through lower main sequence, to giant stars (Skumanich 1972; Noyes et al. 1984; Baliunas et al. 1995; Güdel, Guinan & Skinner 1997; Kitchatinov & Rüdiger 1999; Brandenburg & Dobler 2002). Zahn (1977) and Kopal (1968) have shown that stars with convective envelopes that are members of close binaries have their orbital and rotational periods synchronized by tidal forces. Thus, the tidal forces become additional factors for controlling rotation and atmospheric properties of companions. The binary systems like BY Draconis (BY Dra) type, RS CVn type, W UMa type and Algol which are tidally locked at fast rotation by a close companion are also strongly magnetically active (Berdyugina 2005).

The physics of stellar magnetic activity is not well understood as no spatial information can directly be resolved through observation. Therefore, indirect techniques e.g. Doppler imaging has been extensively used for study of starspots. In this technique high-resolution spectral line profile of rotating stars is used for mapping the stellar surface; proposed first by Deutsch (1958). Thereafter, inversion technique with minimization was developed by Goncharskii et al. (1977). In due course, when the periodic photometric variability of late-type active stars was interpreted as rotational modulation due to the presence of cool spots on their surface, this inverse technique was applied to the spectra of cool stars by Vogt & Penrod (1983). Later numerous subsequent contributions were made by Rice, Wehlau & Khokhlova (1989), Strassmeier et al. (1991), Collier Cameron (1992), Kürster (1993), Unruh & Collier Cameron (1995), Piskunov & Kochukhov (2002) and Donati et al. (2006).

⋆E-mail: patelmanoj79@gmail.com

The high resolution and high signal-to-noise ratio spectroscopic observations with a good phase coverage as required for Doppler imaging are limited, therefore, long-term traditional photometric observations are important to understand the active region evolution and the stellar activity cycles (e.g. Oláh et al. 1997; Pandey et al. 2005a,b; Savanov 2010). We have adopted an inversion code (IPH), which is a published Doppler-imaging inversion code based on quasi-optimal filtering of the objects principal components, developed by Savanov & Strassmeier (2005). This code reconstructs the stellar surface spot configuration from the light curve of a rotating star. They apply it for the first time to a decade-long time series of precise *V*- and *I*-band photometric data of the spotted star V1355 Ori (Savanov & Strassmeier 2008). In order to understand the physical origin of activity, the time-scale of variability and to have a comparison with other similar systems, we have carried out a multiwavelength study of V1147 Tau, a typical late-type system at different levels of activity.

In this paper, we have analysed optical photometric, polarimetric, spectroscopic and *ROSAT* X-ray data of a less well studied K5V-type binary star V1147 Tau. This star was first identified in the *Einstein* Slew Survey, 1ES 0429+130, as a likely optical counterpart of a soft X-ray (0.2–4.0 keV) source with an X-ray flux of $6.5 \pm 2.8 \times 10^{-12}$ erg s^{-1} cm^{-2} (Elvis et al. 1992; Schachter et al. 1996). It was re-discovered in the *ROSAT* All-Sky Survey (RASS) at a somewhat weaker level of $1.38 \pm 0.14 \times 10^{-12}$ erg s^{-1} cm^{-2} and dubbed as 1RXS J043225.9+130648 in the RASS Bright Source Catalog (Voges et al. 1999). The basic parameters of this star, as available from *Hipparcos* satellite are $V = 11.00$ mag, $(B - V) = 1.19 \pm 0.01$ mag and a parallax of 17.55 ± 2.97 mas (Perryman et al. 1997). It has been classified as a BY Dra-type variable in the 74th special name-list of variable stars (Kazarovets et al. 1999). Stauffer et al. (1997) and Bender & Simon (2008) have found this star system to be a single-lined spectroscopic binary. Griffin (2012) has made use of the 92 radial velocities data available from Palomer, OHP CORAVEL and Cambridge, spanning the period from 1997 February to 2005 January and has obtained the orbit of the star system with an orbital period of 1.4846984 ± 0.0000003 d and determined the mass function of about 0.05. Noting that V1147 Tau is a K5V star system, he estimated mass of the primary to be about 0.7 $M_\odot$, whereas of the secondary should be at least 0.4 $M_\odot$. This assigns the secondary a spectral type no later than M2, and 2.5 mag fainter in *V*-band. Griffin has also found, for the first time, a value of the inclination of the orbit about $i \sim 62^\circ$.

The paper is organized as follows. In Section 2 we provide the different sets of observations and data reduction, while the photometric light curve and period analysis of V1147 Tau are given in Section 3. In Section 4 we have modelled the optical light curves observed at different epochs, while Section 5 represents the chromospheric emission feature. In Section 6 we give detailed analysis of the sources of polarization in V1147 Tau, and in Section 7 we describe the X-ray light curve and spectra. In Section 8 we derived stellar parameters, kinematics and age, and in Section 9 we give our discussion and summary.

2 OBSERVATIONS AND DATA REDUCTION

2.1 Optical photometry

V1147 Tau was observed in the *B*, *V*, *R* and *I* filters for 33 nights during the years 2000–2003 and 2009–2011 at Aryabhatta Research Institute of observational Sciences (ARIES), Nainital. The observations were taken with the 104-cm Sampurnanand Telescope (ST) at f/13 Cassegrain focus using a 2k × 2k CCD camera. The CCD system consists of $24 \times 24\,\mu m^2$ size pixel. The CCD covers a field of view $\sim 13 \times 13$ arcmin^2 and the readout noise and gain of the CCD are, respectively, 5.3e$^-$ and 10e$^-$ ADU^{-1}. On each night, a few CCD frames of object field were taken in each filter with exposure times ranging from 10 to 300 s, depending upon the seeing conditions and the filters used. Several bias and twilight flat frames were also taken during each observing run. Bias subtraction, flat-fielding and aperture photometry were performed using IRAF.[1]

In order to get the standard magnitude of the program star, differential photometry has been adopted, assuming that the errors introduced due to colour differences between comparison and program stars are much smaller than the zero-point errors. We have chosen HD 286840 (F8D) and HD 286838 (A7D) as the comparison and check stars. We have also done the photometric calibration of the V1147 Tau field using the Landolt standard field SA98 on 2011 January 1. Our calibration provides $B = 12.313 \pm 0.005$, $V = 11.093 \pm 0.003$, $R = 10.318 \pm 0.002$ and $I = 9.925 \pm 0.002$ mag for V1147 Tau, $B = 11.934 \pm 0.003$, $V = 11.235 \pm 0.003$, $R = 10.804 \pm 0.002$ and $I = 10.341 \pm 0.002$ mag for comparison star HD 286840 and $B = 12.261 \pm 0.004$, $V = 11.498 \pm 0.003$, $R = 11.009 \pm 0.003$ and $I = 10.486 \pm 0.002$ mag for check star HD 286838. The differences in the measured *B*, *V*, *R* and *I* magnitudes of comparison and check stars do not show any secular trend during our observations. The nightly mean of standard deviation of these differences are 0.008, 0.007, 0.006 and 0.008 in the *B, V, R* and *I* bands, respectively. This indicates that both the comparison and check stars were constant during the observation run.

We have supplemented our data with the observations available in *Hipparcos* (Perryman et al. 1997) and in All Sky Automated Survey (ASAS; Pojmaski 2002). In the ASAS observations, we have used only 'A' and 'B' graded data. *Hipparcos* observations spanned 2.5 yr from 1990 January 21 to 1992 July 27. However, the ASAS survey has a much longer span of *V*-band photometry of ∼7 yr (2002 December 13–2009 November 20). Thus the total time-span of the available data set in the *V* band is ∼20 yr with a gap of ∼8 yr from year 1992 to year 2000. This large time base of the observations is useful to study the evolution of spots on the stellar surface.

2.2 Optical spectroscopy

Spectroscopic observations were carried out on 2003 January 24 at the Vainu Bappu Observatory, Kavalur, with the Optomechanics Research (OMR) spectrograph fed by the 234-cm Vainu Bappu Telescope (Prabhu, Anupama & Surendiranath 1998). The data were acquired with a 1k × 1k CCD camera of 24 μm^2 pixel size, covering a range of 1200 Å and having a dispersion of 1.25 Å pixel^{-1}. The spectra have been extracted using the standard reduction procedures in the IRAF packages (bias subtraction, flat-fielding, extraction of the spectrum and wavelength calibration using arc lamps). The spectral resolution was determined by using emission lines of arc lamps taken on the same night and found to be 2.7 Å at 6300 Å ($R \sim 2333$).

[1] http://iraf.net

Table 1. Observed polarized and unpolarized standard stars.

	Polarized standard				Unpolarized standard	
	Schmidt et al. (1992)		This work		This work	
Filter	P (per cent)	θ (°)	P (per cent)	θ (°)	q (per cent)	u (per cent)
	HD 236633				β Uma	
B	5.532 ± 0.040	92.53 ± 0.21	5.485 ± 0.116	92.24 ± 0.58	−0.049 ± 0.060	−0.082 ± 0.061
V	5.485 ± 0.016	93.76 ± 0.08	5.470 ± 0.088	93.31 ± 0.46	0.021 ± 0.056	−0.005 ± 0.056
R	5.376 ± 0.028	93.04 ± 0.15	5.200 ± 0.074	92.37 ± 0.41	0.020 ± 0.062	0.142 ± 0.062
I	4.805 ± 0.036	93.14 ± 0.21	4.498 ± 0.092	92.53 ± 0.57	0.001 ± 0.077	0.069 ± 0.077
	BD+59°389				θ Uma	
B	6.345 ± 0.035	98.14 ± 0.16	6.359 ± 0.124	98.33 ± 0.55	0.044 ± 0.080	0.125 ± 0.080
V	6.701 ± 0.015	98.09 ± 0.07	6.795 ± 0.117	98.54 ± 0.49	−0.048 ± 0.073	0.086 ± 0.073
R	6.430 ± 0.022	98.15 ± 0.10	6.558 ± 0.109	98.76 ± 0.47	0.062 ± 0.064	−0.093 ± 0.065
I	5.797 ± 0.023	98.26 ± 0.11	5.767 ± 0.115	99.22 ± 0.56	−0.061 ± 0.087	−0.124 ± 0.086
	HD 19820				HD 14069	
B	4.699 ± 0.036	115.70 ± 0.22	4.491 ± 0.092	116.21 ± 0.58	−0.011 ± 0.032	−0.061 ± 0.032
V	4.787 ± 0.028	114.93 ± 0.17	4.825 ± 0.105	115.58 ± 0.61	0.076 ± 0.046	−0.158 ± 0.046
R	4.526 ± 0.025	114.46 ± 0.16	4.575 ± 0.099	112.82 ± 0.61	−0.040 ± 0.047	−0.093 ± 0.047
I	4.081 ± 0.024	114.48 ± 0.17	4.143 ± 0.106	114.36 ± 0.72	0.034 ± 0.049	−0.126 ± 0.049

2.3 Optical polarimetry

The B, V, R and I broad-band polarimetric observations of V1147 Tau were obtained on 2010 December 27–28 and 2011 November 17 using ARIES Imaging Polarimeter (AIMPOL) mounted on the 104-cm Sampurnanand Telescope of ARIES, Nainital. The detailed descriptions about the AIMPOL, data reduction, calculations of polarization and position angle are given in Rautela, Joshi & Pandey (2004). For calibration of polarization angle zero-point, we have observed highly polarized standard stars, and the results are given in Table 1. Both the program and the standard stars were observed during the same night. The obtained values of polarization and position angles for standard polarized stars are in good agreement with Schmidt, Elston & Lupie (1992). To estimate the value of instrumental polarization, unpolarized standard stars were observed. These measurements show that the instrumental polarization is below 0.1 per cent in all pass bands (see Table 1). In fact, the instrumental polarization of ST has been monitored since 2004 within other projects as well (e.g. Medhi et al. 2007, 2008; Pandey et al. 2009). These measurements demonstrated that it is invariable in all B, V and R passbands. The instrumental polarization was then applied to all measurements.

2.4 Archival X-ray data

V1147 Tau was observed serendipitously in pointed observations of the *ROSAT* Photon Sensitive Proportional Counter (PSPC) for five occasions for 17.4 ks (obs ID: rp200553n00; epoch 'a'), 4.1 ks (obs ID: rp200945n00; epoch 'b'), 7.4 ks (obs ID: rp200942n00; epoch 'c'), 11 ks (obs ID: rp200911n00; epoch 'd') and 13.7 ks (obs ID: rp200911a01; epoch 'e') from 1992 February 27 (UT 17:20:26) to 1993 March 3 (UT 11:12:49). The offset of the observations was 45.9 arcmin during the epochs a, d and e, 44.8 arcmin during the epoch b and 52.6 arcmin during the epoch c. The PSPC had an energy range of 0.1–2.4 keV with a low spectral resolution ($\Delta E/E \approx 0.42$ at 1 keV). A full description of the X-ray telescope and detectors can be found in Trümper (1983) and Pfeffermann et al. (1987). X-ray light curves and spectra of the star V1147 Tau were accumulated from on-source counts obtained from circular regions on the sky centred on the X-ray peaks. The light curves for the source and background were extracted using the XSELECT package for the 0.2–2.4 keV energy band of PSPC which contains all the X-ray photons. The background was accumulated from several neighbouring regions at nearly the same offset as the program star.

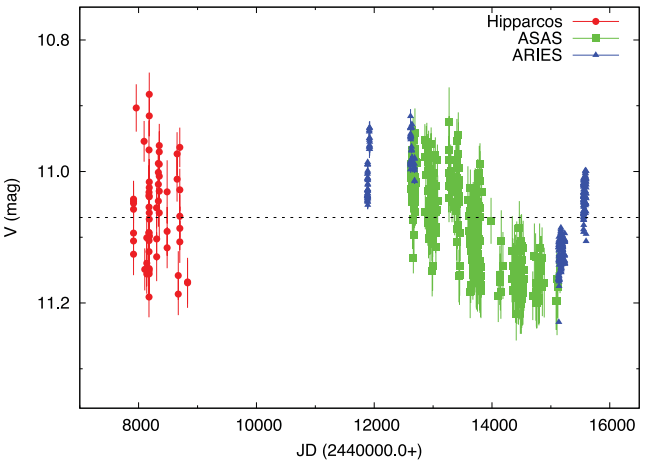

Figure 1. 20 yr V-band light curve of the star V1147 Tau. The mean V-band level is plotted by dotted line.

3 PHOTOMETRIC LIGHT CURVE AND PERIOD ANALYSIS

Fig. 1 shows the light curve of V1147 Tau in V band compiled from different observations. The photometric data have high amplitude, both short-term and long-term, variations. The short-term variations are clearly due to rotational modulation, while the long-term variation is likely due to some sort of multiperiodic spot cycle. Large gaps in the data set led to complications in the interpretation of the power density spectrum, as the true frequencies of the source were further modulated by the irregular and infrequent sampling defined by the window function of the data. Therefore, we

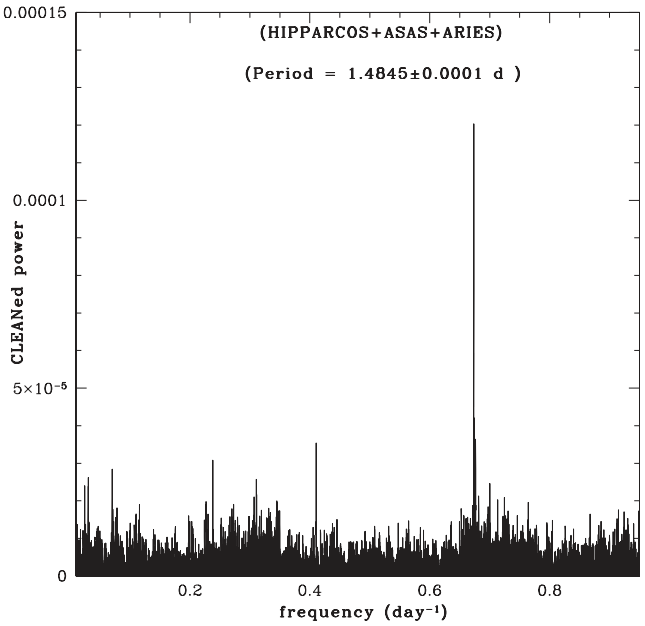

Figure 2. CLEANed power spectrum of the light curve shown in Fig. 1.

have used the one-dimensional CLEAN algorithm (Roberts, Lehar & Dreher 1987) as implemented in the UK STARLINK PERIOD package (Dhillon, Privett & Duffey 2001). In the CLEAN algorithm, the discrete Fourier transform first calculated from the light curve is followed by the deconvolution of the 'window' function from the data. Despite the noise and the fact that the light curve is not exactly sinusoidal, the power spectrum picks out the rotation period (Bailer-Jones & Mundt 2001). Fig. 2 shows the CLEANed power spectrum of the entire data set shown in Fig. 1. The CLEANed spectrum was obtained after 100 iterations with a loop gain of 0.1. The highest peak in the CLEANed spectrum corresponds to a period of 1.4845 ± 0.0001 d. The uncertainty in the period is defined as $P^2/(2t_{\max})$, where P is the period and $t_{\max}$ is the duration of the observation (Roberts et al. 1987). It is important to remark that Delorme et al. (2011) have obtained the rotational period of 1.48 d, whereas Bender & Simon (2008) and Griffin (2012) have obtained the orbital period of 1.4847 d. This indicates that the system is in synchronous rotation.

The activity of cool stars affects the overall properties of the photosphere of a star in its intrinsic mean colours. Therefore, in Fig. 3 we have plotted the $(B - V)$, $(V - R)$ and $(V - I)$ colour curves along with the V magnitude as a function of rotational phase. Small variations were observed in these colours. We have obtained the correlation of the variations in colours with the V-band light curve. The correlation coefficients between $(B - V)$ and V, $(V - R)$ and V and $(V - I)$ and V were found to be 0.18, 0.64, 0.85 along with probability of no correlation of 0.00319, 9.8×10^{-31} and 0, respectively. The correlation between the colour index and V-band variation increases with a wider colour baseline, indicating that the variations are due to the presence of cool starspots. Generally, an active star is redder at its minimum brightness, in agreement with the hypothesis of cool starspots as the cause of the photometric variations. However, evidence of $B - V$ and, more strongly, $U - B$ colour curves being anticorrelated with the V-band light curve have been provided for very active systems, like UX Ari and HR 1099 (Catalano et al. 1996) and MM Her (Tas, Evren, Ibanoğ 1999) indicating the presence of a distribution of hotspots (plages, faculae, prominences and flares) on the photosphere of the star.

4 LIGHT-CURVE INVERSION

We employ the light-curve inversion code (IPH) of Savanov & Strassmeier (2008) and Savanov (2009). The inversion code reconstructs the distribution of temperature inhomogeneities on the stellar surface from the observed light curve in a two-temperature approximation (the temperatures of the unperturbed photosphere and the spots are used as inputs). This technique is based on the same inversion principles as the Doppler imaging technique. It does not make any assumption about the number, shapes or position of the restored temperature inhomogeneities. In the past similar technique was being used by several authors (e.g. Lanza et al. 1998; Berdyugina, Pelt & Tuominen 2002; Korhonen, Berdyugina & Tuominen 2002). In our modelling, the surface of the star was divided into $6^\circ \times 6^\circ$ pixels (unit areas). For each pixel filling factors f were determined as part of the solution. The unknown parameter photospheric spot filling factor is a composite of a two-temperature contribution; the intensity from the photosphere (I_P) and from cool spots (I_S) weighted by the fraction f of the surface covered with spots. The intensity per pixel is then given by

$$I = f\, I_P + (1 - f)\, I_S \quad (1)$$

with $0 < f < 1$. The inversion produces a distribution of f over the visible stellar surface that reproduces the data more accurately. The broad-band fluxes as input for model were calculated using atmospheric models from Kurucz (2000). Opposite to spectral line profiles for Doppler imaging, the photometric light curves represent only one-dimensional time series, therefore, reconstructed stellar image contains only poor/no information about stellar latitude. Similar to other light curve inversion codes, our code also suffers from little to no latitudinal information. This inversion code was also used in the past by Strassmeier et al. (2008), Savanov (2009, 2010) and Savanov & Dmitrienko (2011).

In order to model the entire light curve, all observations in V band were divided into 16 sets without gaps on the curve on the phase diagram and without changes of its shape. Each individual light curve was analysed using the IPH code. Fig. 4 shows the results of reconstructing the temperature inhomogeneities on the surface of V1147 Tau for 16 sets of observations. Taking into consideration the available photometric data and the calibration due to Torres, Andersen & Giménez (2010), we took the temperature of the V1147 Tau photosphere to be 4900 K, and the temperature of the spots to be 1000 K lower (Berdyugina 2005). We have made use of the data from the Kurucz's model grid in our computations. The angle of inclination (i) for V1147 Tau was derived to be $\sim 60^\circ$ (Griffin 2012), therefore, reconstruction of the temperature-inhomogeneity maps was carried out for $i = 60^\circ$. The difference in i was reflected only in the resulting fractions of the stellar surface covered by spots. Further, the numerical light-curve simulations by Savanov & Strassmeier (2008) demonstrated that a change in the inclination angle of even $\pm 15^\circ$ marginally altered the light-curve solution. The resulting parameters for the $i = 60^\circ$ are given in Table 2.

From computed maps, we determined the longitudes corresponding to the maximum values of f (dark regions in Fig. 4). The spots have tendency to concentrate at two longitudes, the corresponding values were registered as two independent active regions (longitudes). Fig. 5(b) shows the plot between active longitudes and mean epoch of observations. The difference between two active longitudes was not found to be constant at 180°. This difference was

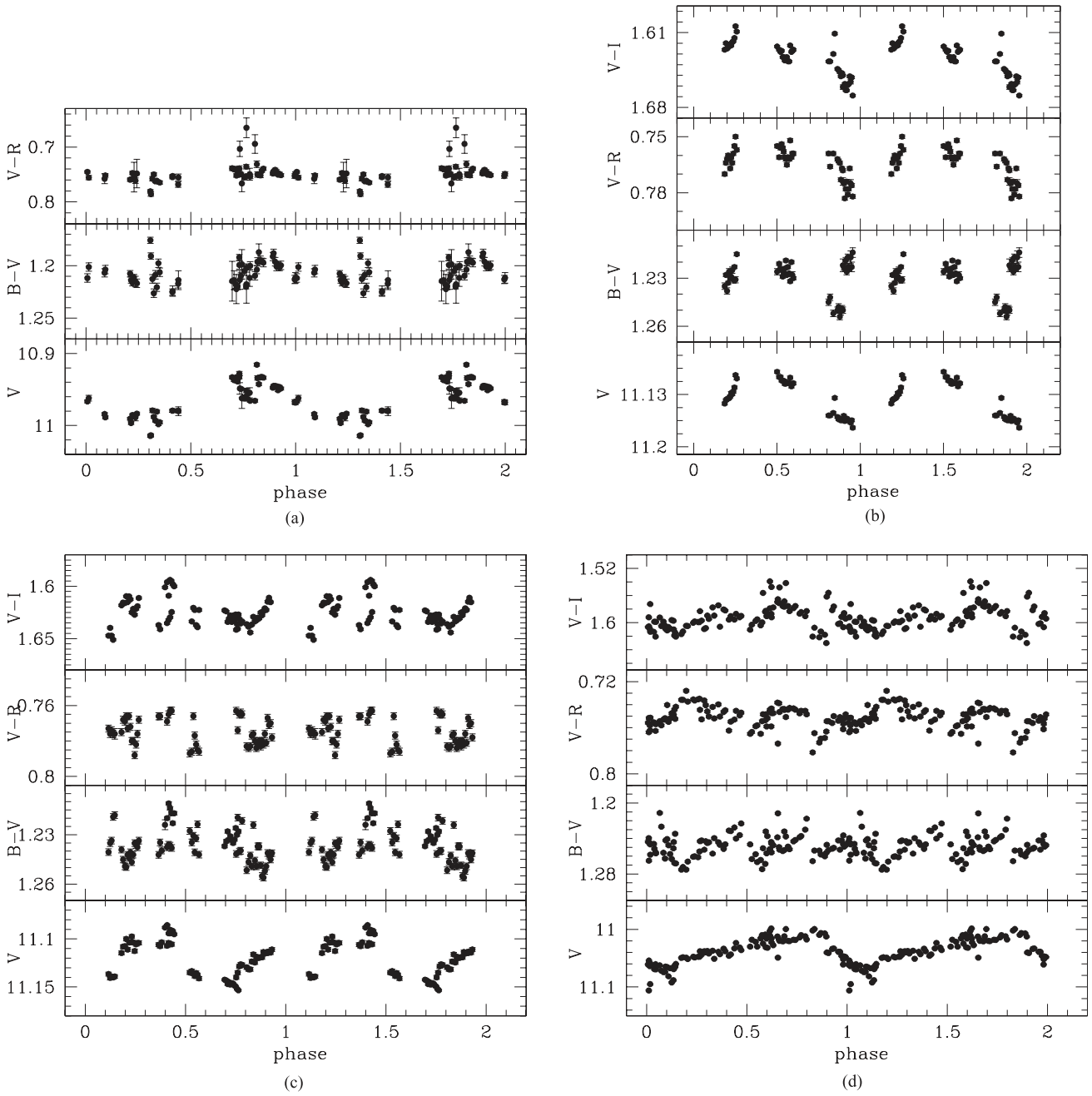

Figure 3. The $B - V$, $V - R$ and $V - I$ colour curves along with the V-band light curve during the epochs (a) '3', (b) '13', (c) '14' and (d) '15' as shown in Fig. 4.

found up to 210°. There may be uncertainties in location of active longitudes due to incomplete light curve or gaps in the phase of light curve. The uncertainty in the positions of the active longitudes on the stellar surface was on average of about 6° (or 0.02 in phase). The active regions with equal sizes and uncertain position are represented by rombs in Fig. 5(b). The horizontal dashed straight lines in Fig. 5(b) represent the two groups of active longitudes.

Stars with long enough data show a back and forth of activity within two active longitudes 180° apart with alternate levels of spot activity. This phenomenon is commonly known as flip-flop. The average time between such flip-flops is referred to as flip-flop cycle and has been observed to be in the range of a few years to a decade. The flip-flop events were detected in both light-curve variations and Doppler images (Berdyugina & Tuominen 1998; Berdyugina et al. 1998). Recently, Berdyugina (2005, 2007) has given an observational overview of such cycles. We have also noticed similar events in V1147 Tau. The shaded region in Fig. 5(b) corresponds to time intervals when the possible flip-flop event occurs, i.e. the longitude of the more active region was changed by phase of ∼0.5. The observed flip-flop event of V1147 Tau appears to be related to the extrema of the light curve amplitudes, but it started slightly after the maximum of the light curve, and ends before the minimum. In the photometric light curve modelling, the change in latitude of spots may falsely give apparent switching of active longitude. However, Doppler imaging technique, which restores the polar and near-polar spots with high quality, did not register huge drifts in latitudes (e.g.

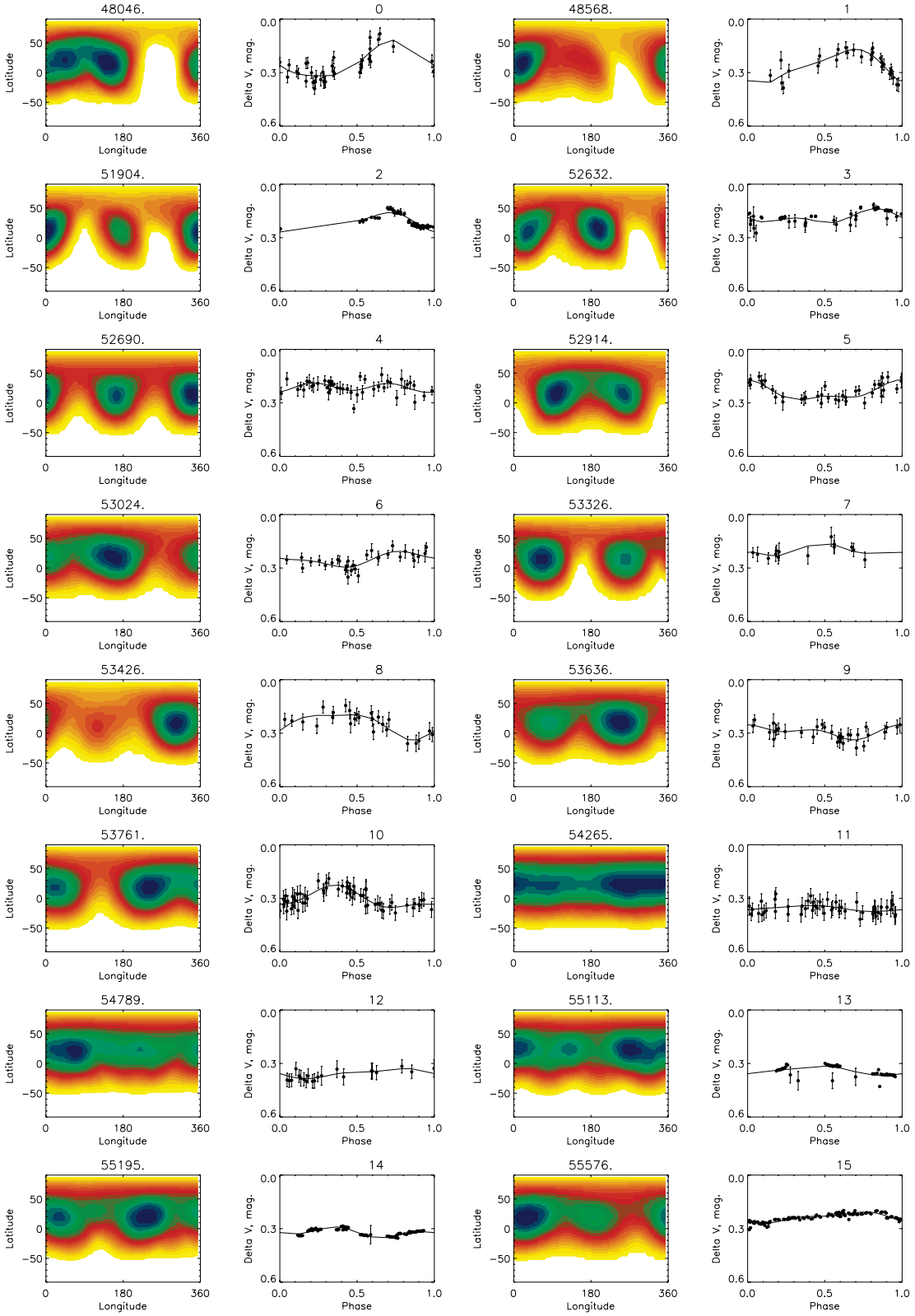

Figure 4. The temperature inhomogeneities map on the surface of V1147 Tau for 16 sets of observations. The map was carried out for $i = 60^{\circ}$. The surface maps are presented on the same scale, with darker regions corresponding to higher filling factors. Observed and theoretical (derived from the model) light curves are also shown in the corresponding right-hand panel.

Table 2. Parameters derived from light-curve modelling.

Data set	No. of points	HJD_{beg} (240 0000.0+)	HJD_{end} (240 0000.0+)	HJD_{middle} (240 0000.0+)	V_{max} (mag)	V_{min} (mag)	V_{mean} (mag)	A (mag)	S_p (per cent)	ψ_1 (°)	ψ_2 (°)	Note[a]
0	35	47913.47	48180.15	48046.81	10.883	11.191	11.069	0.308	13.581	147	50	e
1	27	48305.20	48830.85	48568.02	10.961	11.186	11.056	0.226	15.699	22	150	e
2	51	51884.26	51924.30	51904.28	10.934	11.051	11.003	0.117	10.688	0	...	u
3	49	52615.19	52650.59	52632.89	10.916	11.074	10.979	0.158	9.778	202	37	e
4	47	52655.56	52724.50	52690.03	10.942	11.132	11.010	0.190	11.739	350	168	e
5	38	52859.93	52968.71	52914.32	10.952	11.103	11.031	0.151	13.819	100	260	n
6	30	52971.66	53077.50	53024.58	10.975	11.151	11.058	0.176	14.618	160	367	n
7	14	53266.84	53385.63	53326.24	10.925	11.054	11.007	0.129	10.651	65	266	u
8	25	53394.60	53457.49	53426.04	10.945	11.159	11.041	0.214	14.250	310	122	n
9	32	53591.93	53680.73	53636.33	11.025	11.183	11.098	0.158	17.516	253	83	n
10	58	53700.65	53822.48	53761.57	10.989	11.182	11.100	0.193	18.215	248	20	n
11	51	53983.86	54547.50	54265.68	11.075	11.217	11.157	0.142	22.066	277	5	n
12	21	54691.92	54886.56	54789.24	11.116	11.200	11.167	0.084	21.874	68	255	n
13	53	55088.87	55138.46	55113.66	11.100	11.229	11.143	0.130	20.913	278	10	u
14	74	55155.73	55235.24	55195.48	11.086	11.153	11.121	0.068	19.708	242	32	e
15	100	55554.15	55598.27	55576.21	10.999	11.106	11.039	0.107	13.493	27	188	n

Notes. ψ_1 and ψ_2 are active longitudes; A is amplitude of variability; V_{max}, V_{min} and V_{mean} are maximum, minimum and mean magnitudes of the V1147 Tau.

[a]e – size of both spots were approximately equal; n – size of both spots were not equal; u – uncertain result due to incomplete light curve.

Berdyugina et al. 1998). In any case, it is to be kept in mind that overinterpreting image reconstruction from light curves will require utmost care.

The total area covered by spots (Sp) was on an average 18 per cent of the total visible stellar surface. During the observations the value of spottedness varied in the range 9–22 per cent for the inclination of 60° (see Fig. 5c). As seen in Fig. 5(d) the amplitude of the brightness variations decreased slightly from 0.3 to 0.06 mag. Both amplitude and spottedness have variations on time-scales of about ∼4000 d. Fig. 5(e) shows the variation of minimum, maximum and mean brightness of the star V1147 Tau.

The secondary in V1147 Tau system is 2.5 mag fainter than the primary (Griffin 2012). Thus, the secondary will contribute negligible flux to the system. Therefore, we have performed the modelling on the assumption that the activity is only due to the primary component of the system. The effect of binarity has been also calculated employing the data from Bender & Simon (2008) adopting masses of the components as 0.79 and 0.58 $M_\odot$. The contribution from the secondary has been taken into account using traditional approaches starting from Vogt (1981). We have found that the binarity increases the value of spottedness by 4–5 per cent as the subtraction of the secondary increases the contrast of the light variability of the primary. However, the geometry and evolution of active regions remain unaffected.

5 CHROMOSPHERIC EMISSION FEATURE

In late-type dwarfs, Hα emission is a good indicator of chromospheric activity. It has been suggested that the detection of Hα emission above the continuum or even a filled in emission is sufficient to indicate that a K-M dwarf is a BY Dra variable (Bopp et al. 1981). Only the very active stars show Hα emission above the continuum, whereas in less active stars only a filled in absorption line is observed. Hα line for some objects goes from filled in absorption to emission during the flare events (Catalano & Frasca 1994). The spectrum of V1147 Tau in the Hα regions is shown in Fig. 6. The emission in Hα is clearly seen in the spectra. The equivalent width of the Hα emission line is found to be 1.52 Å. This is similar to the equivalent width found (1–2 Å) for BY Dra-type stars (Bopp 1987). The equivalent width of Hα for a similar single-lined spectroscopic binary BK Psc (spectral type: K5V+M3V) has been found in the range 1.09–1.70 Å (see Gálvez et al. 2002). A strong Hα emission feature has been also found in many other similar type stars e.g. HD 160934 (Mullis & Bopp 1994) and FR Cnc (Pandey et al. 2005a; Golovin et al. 2012).

6 SOURCES OF POLARIZATION

The values of polarization and polarization position angle of V1147 Tau as observed at three different epochs are given in Table 3. The values of degree of polarization appear to be constant during observations. However, the polarization in *B* band during 2010 December 27 observations was found to be large with respect to the other two observations. The mean values of degree of polarization and polarization position angle were calculated to be 0.40 ± 0.03, 0.22 ± 0.05, 0.17 ± 0.07 and 0.12 ± 0.04 per cent, and $71° \pm 5°$, $85° \pm 5°$, $73° \pm 9°$ and $80° \pm 6°$ in *B, V, R* and *I* bands, respectively.

Being a nearby star (distance = ∼45 pc), V1147 Tau may suffer negligible reddening. Therefore, observed polarization in V1147 Tau cannot be foreground in origin. The polarization in V1147 Tau was found to be similar to that of solar-type stars (see e.g. Scalitriti et al. 1993; Alekseev & Kozlova 2003). Similar to the most of active stars, the observed polarization in V1147 Tau was found to decrease towards longer wavelengths (e.g. Yudin & Evans 2002; Rostopchina et al. 2007). This could be due to selective absorption by circumstellar dust, which decreases towards longer wavelengths. As a result, the ratio of the intensity of the polarized light (i.e. scattered) to the intensity of unpolarized light (i.e. stars light coming directly to us) decreases with increasing wavelength of the radiation. Another possible reason may be wavelength-dependent albedo of reflected light from the circumstellar material, which decreases towards longer wavelengths resulting in less scattering and thus polarization. The mechanism of the polarization in late-type dwarf stars has been also interpreted by magnetic intensification or scattering by circumstellar material.

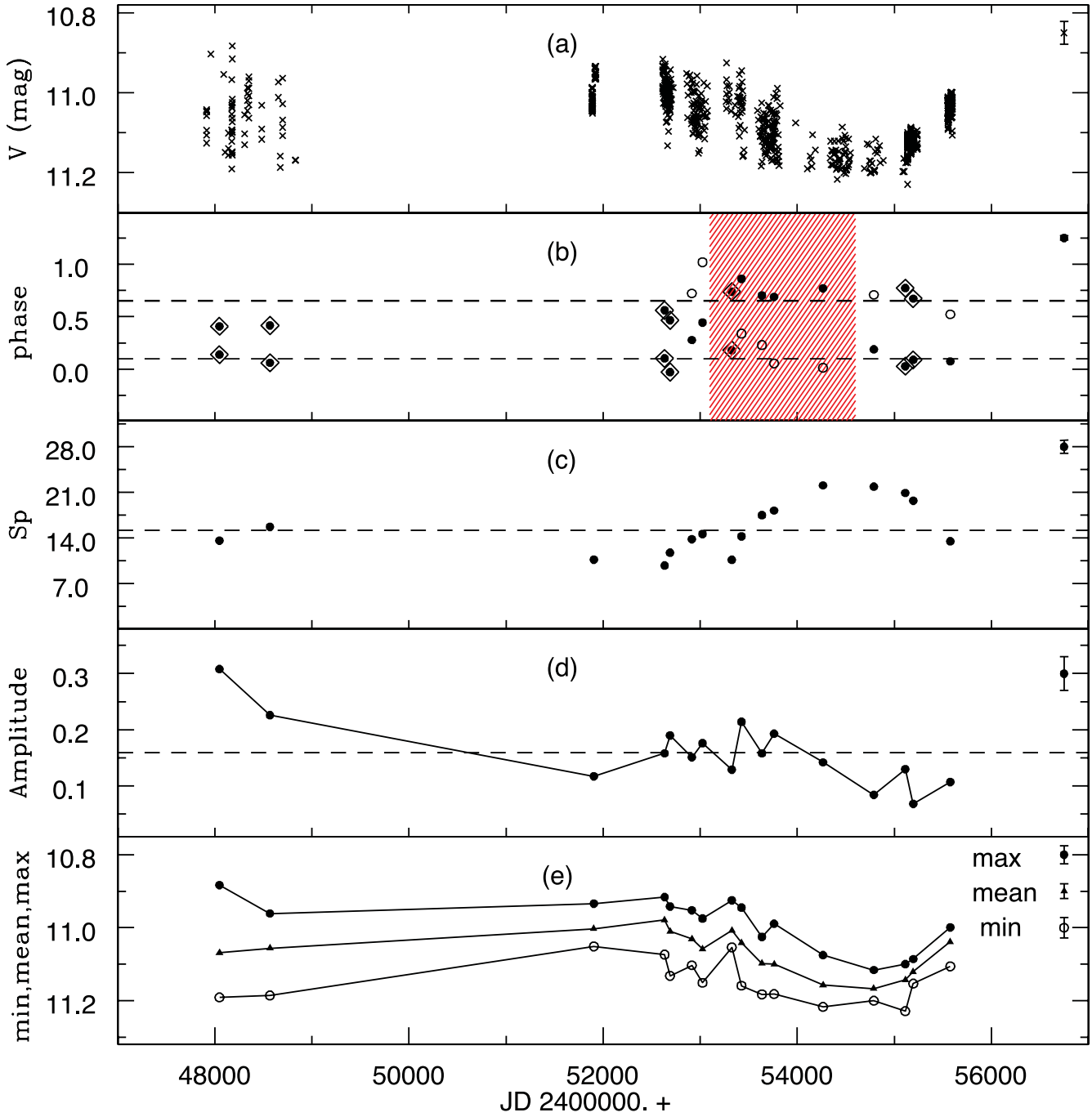

Figure 5. (a) *V*-band light curve of V1147 Tau. (b) Phases of active longitudes: filled and open circles show high and low active regions, rombs show the equal size spots with uncertain position and shaded region shows the time intervals when the possible flip-flop event occur. (c) Variations of the spottedness of the surface of V1147 Tau. (d) Variations of the brightness amplitude. (e) Variations of the mean, minimum and maximum brightness amplitudes for each set of observations. Mean error bars are shown above right-hand corner on each panels. Error in panel (b) is less than the size of the symbols.

Huovelin & Saar (1991) and Saar & Huovelin (1993) showed that the degree of polarization depends non-linearly on the size of cool spots on the surface of star. Saar & Huovelin (1993) have calculated a grid of expected degrees of polarization in *U, B, V, R* and *I* bands for the stars with temperature from 4000 to 7000 K, log *g* from 2.0 to 4.5 and total spot area of 24 per cent. They have calculated the maximum possible degree of polarization for stars of spectral type K5-7V and with characteristic magnetic field 2.7 kG. In our modelling, we have found the maximum spottedness of V1147 Tau to be 22 per cent. The degree of polarization in *B, V, R* and *I* bands with their theoretical values are shown in Fig. 7, where the theoretical values are represented by a continuous line. The observed polarization in all bands exceeds slightly the theoretical values expected for a Zeeman polarization model. A similar trend has also observed in some other young spotted stars viz. FR Cnc (Golovin et al. 2012), LO Peg (Pandey et al. 2009), MS Ser, LQ Hya and VY Ari (Alekseev 2003). This is probably due to the presence of a supplementary source of linear polarization (e.g. see Pandey et al. 2009). The

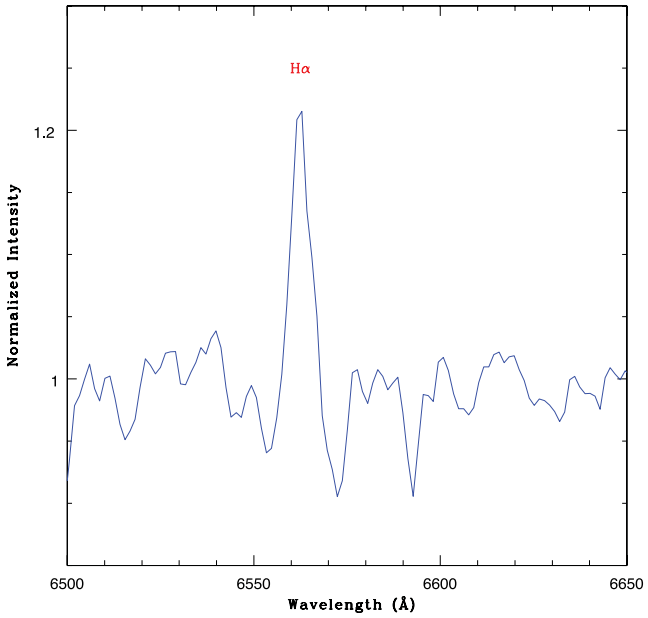

Figure 6. Hα spectrum of the V1147 Tau.

Table 3. Observed *BVRI* polarization values for V1147 Tau.

Date of observation	Filter	P (per cent)	θ (°)
2010 December 27	*B*	0.54 ± 0.01	79 ± 2
	V	0.22 ± 0.01	78 ± 2
	R	0.25 ± 0.08	83 ± 3
	I	0.16 ± 0.05	95 ± 6
2010 December 28	*B*	0.34 ± 0.09	78 ± 6
	V	0.21 ± 0.08	94 ± 8
	R	0.12 ± 0.04	69 ± 11
	I	0.11 ± 0.06	74 ± 10
2011 November 17	*B*	0.33 ± 0.06	57 ± 8
	V	0.24 ± 0.07	82 ± 6
	R	0.13 ± 0.10	68 ± 12
	I	0.09 ± 0.01	70 ± 3

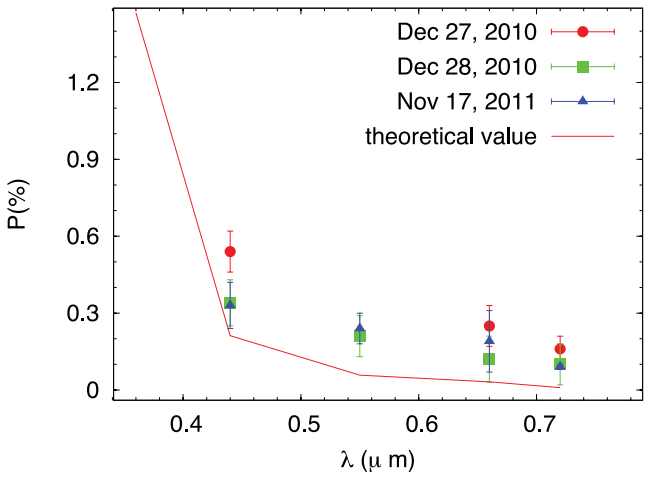

Figure 7. Degree of polarization as a function of wavelength observed at different epochs. The continuous line shows the theoretical values of the degree of polarization expected for a Zeeman polarization model.

excess in observed polarization could not be explained by predicted values of polarization due to Thompson and Rayleigh scattering from inhomogeneous regions as Thompson and Rayleigh scattering for the assumed spectral type supposed to be of order of 10^{-7} and 10^{-4} per cent, respectively (Saar & Huovelin 1993). Further, V1147 Tau is close binary system, therefore, the mentioned models may not be acceptable (Elias & Dorren 1990; Saar & Huovelin 1993; Alekseev 2003). The additional linear polarization could be due to the scattering in circumstellar material (e.g. see Pandey et al. 2009).

7 X-RAY LIGHT CURVE AND SPECTRA

Fig. 8(a) shows the background subtracted X-ray light curve in the energy band 0.2–2.4 keV along with the *Hipparcos* *V*-band light curve. The temporal binning of the X-ray light curve is 128 s. The X-ray light curve at the start of observation was quasi-simultaneous with the *V*-band light curve from *Hipparcos*. Sudden enhancements in the count rates were observed during epochs 'a', 'b' and 'd', which could probably be due to flaring events as X-ray flaring is quite common in late-type active stars (e.g. see Pandey & Singh 2008, 2012). Because of the low count rate, we could not analyse these flaring structures. Stelzer, Neuhaeuser & Hambaryan (2000) have also detected flares in these epochs and have determined the rise and decay times. Apart from these flaring spikes, the light curves appear to be slowly varying. The χ^2 test has been performed for deviations from the mean count rates to determine the existence of the variability in the light curves for all five epochs separately. The χ^2 test is defined as

$$\chi^2 = \sum_{i=1}^{N} \frac{(C_i - \overline{C})}{\sigma_i}, \qquad (2)$$

where $\overline{C}$ is average count rate, C_i is count rate of ith observations, σ_i is the error corresponds to C_i and N is total number of data points. From the χ^2 test, these observations have been found to be variable with confidence levels of 99.96, >99.99, >99.99, 82.5 and 95.6 per cent for epochs 'a', 'b', 'c', 'd' and 'e', respectively. The entire data were found to be variable with confidence level >99.999 per cent. The χ^2 test was performed after removing the flare spikes. The variation in X-ray light curves could be due to the rotation of the star V1147 Tau itself. Therefore, in order to see the rotational modulation in the X-ray light curve, we have folded the entire X-ray data using the ephemeris HJD = 244 7913.46536+1.4845*E*. Fig. 8(b) shows the folded X-ray light curve of the star V1147 Tau along with the quasi-simultaneous folded *V*-band light curve observed by *Hipparcos* (set '1' as shown in Fig. 1). We have estimated the degree of rotational modulation from the amplitude of a sine wave fit to the data with rotational period. The amplitude of the fitted sine wave was found to be 0.030 ± 0.005 counts s^{-1}. With mean levels of 0.137 counts s^{-1} the derived amplitude corresponds to rotational modulation of 22 per cent. Rotational modulation was also seen in other various active stars e.g. V711 Tau (Agrawal & Vaidya 1988; Audard et al. 2001), AB Dor (Kürster et al. 1997), where the degree of rotational modulation was found up to 30 per cent. The X-ray light curve appears to be anticorrelated with the *V*-band light curve in the sense that during the *V*-band minimum, X-ray maximum was seen. This indicates that the high magnetic regions at the surface of V1147 Tau results in to a high level of X-ray emission.

The X-ray spectra of V1147 Tau, as observed with the *ROSAT* PSPC during three different epochs 'a', 'd' and 'e', are shown in Fig. 9. Response matrices based on the available off-axis calibration

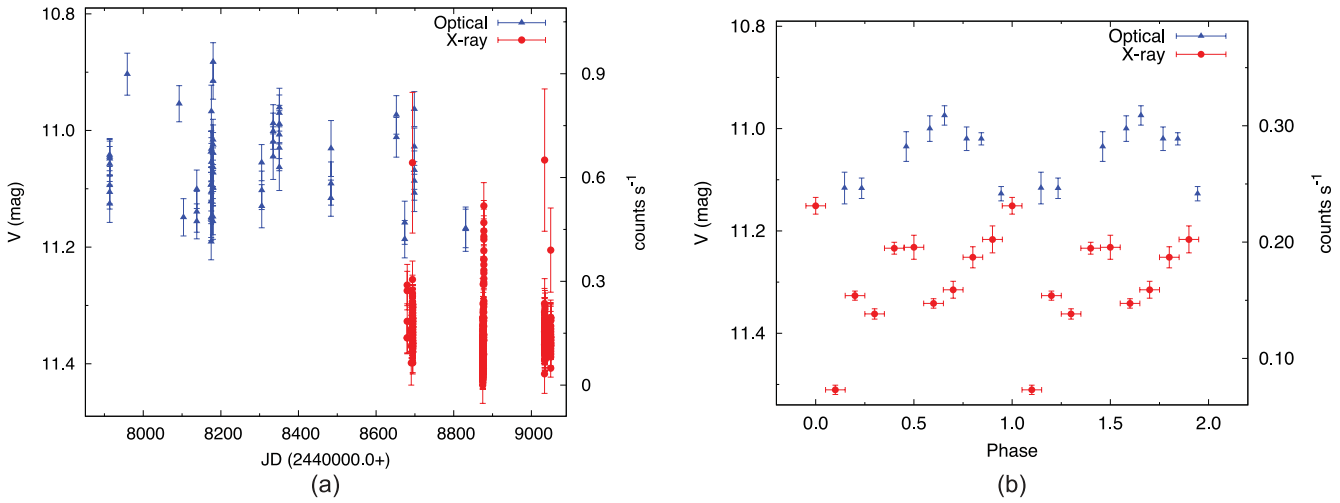

Figure 8. X-ray light curve along with quasi-simultaneous *V*-band light curve from *Hipparcos*.

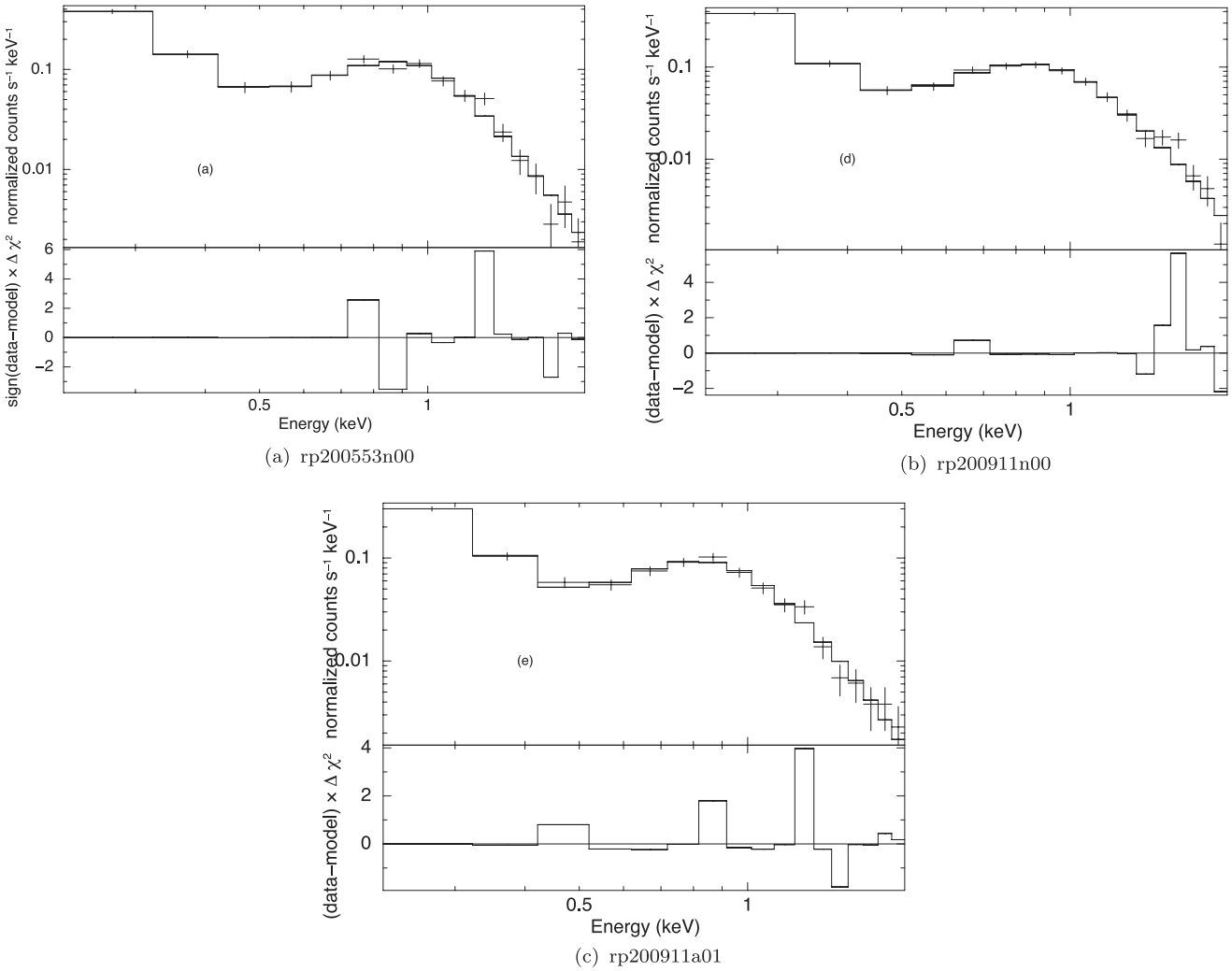

Figure 9. X-ray spectra along with the best-fitting APEC 2T model during epochs a, d and e.

of the PSPC and using the appropriate ancillary response files were created and the data were fitted using the XSPEC (version 12.5.1; Arnaud 1996) spectral analysis package. The background subtracted individual spectra were binned so as to have a minimum of 20 counts per energy bin. The *ROSAT* PSPC spectra of the star V1147 Tau were fitted with single (1T) and two temperature (2T) collisional plasma models known as APEC (Smith et al. 2001), with variable elemental abundances, *Z*. The interstellar hydrogen column density

($N_{\rm H}$) was left free to vary. For each set of the X-ray spectra, no 1T or 2T plasma models with solar photospheric (Anders & Grevesse 1989) abundances ($Z_{\odot}$) could fit the data, as unacceptably large values of χ^2_{ν} were obtained. For each set of data, acceptable APEC 2T fits were achieved only when the abundances were kept fixed at value of 0.1 $Z_{\odot}$. However, the spectral fit could not be performed for the spectral data during epochs 'b' and 'c' due to low count rate as the star was observed for only a short time. The combined spectra were also fitted with the 1T, 2T and 3T APEC model, but no 1T, 2T or 3T plasma models with solar/subsolar photospheric abundances could fit the data well. This could be due to the variable X-ray emission during the different epochs of the observations. The best spectral parameters for each epoch of the observations are given in Table 4. It is clearly seen that hydrogen column density ($N_{\rm H}$) and temperature of cool component (kT_1) were found consistent to within the 1σ level. However, temperature of hot component (kT_2) during the epoch 'a' is 1.5 times more than that found for epochs 'd' and 'e'. The volume emission measure corresponding to cool component (EM_1) is well within a 1σ level for each epoch of observations. However, volume emission measure corresponding to hot component (EM_2) was found two times more during epochs 'd' and 'e' than that for the epoch 'a'. The X-ray luminosity during the epoch 'a' is found to be 6.8×10^{29} erg s^{-1}, which is 1.4–1.5 times more that found during epochs 'd' and 'e'. The high temperature and luminosity during the epoch 'a' could be due to the flaring coronae as seen in the light curve.

8 STELLAR PARAMETERS, KINEMATICS AND AGE

The spectral energy distribution (SED) is important to determine the presence of circumstellar material, spectral type and other basic parameters of the stars. We have determined SED of V1147 Tau by using broad-bands *B*, *V*, *R*, *I* (present photometry), Two Micron All Sky Survey (2MASS) *J*, *H*, *K* (Cutri et al. 2003) magnitudes, *Wide-field Infrared Survey Explorer* (*WISE*) 3.4, 4.6, 12 and 22 μm (Cutri et al. 2012) and Multiband Imaging Photometer for *Spitzer* (MIPS) 24 μm (Cieza, William & Jean-Charles 2008). The observed SED of V1147 Tau along with the synthetic SEDs are shown in Fig. 10. The synthetic SED (Kurucz, private communication) is derived from the intrinsic properties of the star. We have plotted synthetic SEDs for different set of $T_{\rm eff}$ and log *g* combinations. The values of $T_{\rm eff}$ and log *g* which are best matched with the observed SED are 4250 ± 250 K and 4.5 ± 0.5, respectively; consistent with the identification of V1147 Tau as a K5V spectral type star system. The flux at 24 μm appears to be slightly above the synthetic SED indicating the presence of thin circumstellar material around V1147 Tau. However, this could be due to the contribution from companion star.

Table 4. Parameters derived from the X-ray spectral fit.

Data (→) Parameters (↓)	rp200553n00 (a)	rp200911n00 (d)	rp200911a01 (e)
$N_{\rm H}$ (cm^{-2})	$3.28^{+1.7}_{-0.06}$	$3.21^{+0.7}_{-0.05}$	$3.15^{+0.03}_{-0.04}$
Z ($Z_{\odot}$)	0.1 (fixed)	0.1 (fixed)	0.1 (fixed)
kT_1 (keV)	$0.07^{+0.02}_{-0.02}$	$0.07^{+0.02}_{-0.02}$	$0.07^{+0.03}_{-0.02}$
kT_2 (keV)	$0.75^{+0.08}_{-0.07}$	$0.60^{+0.09}_{-0.09}$	$0.67^{+0.06}_{-0.07}$
EM_1 (10^{53} cm^{-3})	$9.7^{+5.2}_{-0.6}$	$9.5^{+4.7}_{-0.7}$	$7.7^{+3}_{-0.7}$
EM_2 (10^{53} cm^{-3})	$0.34^{+0.07}_{-0.07}$	$0.60^{+0.19}_{-0.15}$	$0.67^{+0.12}_{-0.09}$
$L_{\rm X}$ (10^{29} erg s^{-1})	6.8 ± 0.5	4.4 ± 0.9	4.8 ± 0.8
χ^2_{ν} (dof)	1.3 (9)	0.9 (9)	1.0 (9)

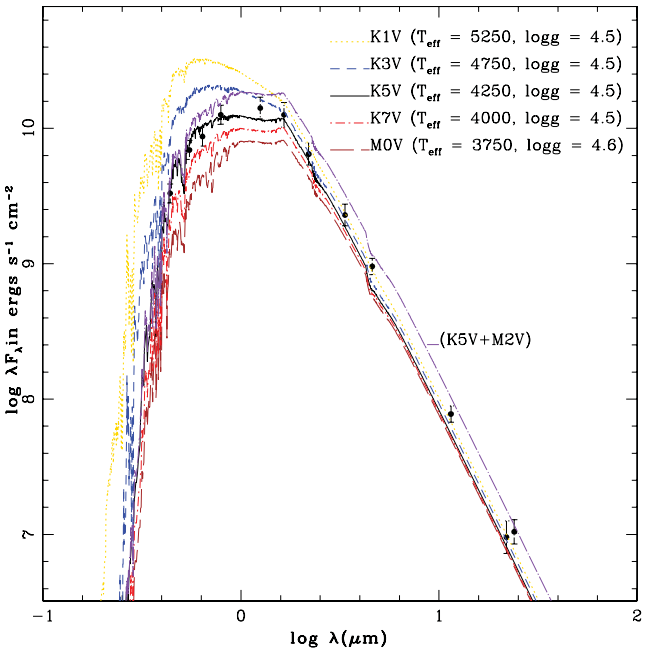

Figure 10. SED of the V1147 Tau along with the synthetic SED for different set of temperature and log *g*. The best-matched $T_{\rm eff}$ = 4250 ± 250 K and log *g* = 4.5 ± 0.5.

In order to see the contribution of binary companion, we have overplotted combined (K5V+M2V) synthetic SED of V1147 Tau. The combined SED is well matched with observed within a 1σ level.

Using the parallax of 22.19 ± 0.71 mas (Röser et al. 2011), interstellar extinction $A_{\rm v}$ = 0.10 (Bobylev, Bajkova & Gontcharov 2006) and the average value of mean magnitude V = 11.07 mag, the absolute magnitude M_V of V1147 Tau is calculated to be 7.70 ± 0.07 mag, which is consistent with a luminosity class V. The intrinsic ($B - V$) colour of V1147 Tau derived from the present photometry is 1.22 ± 0.01. This value of ($B - V$) is best matched with a spectral class of K5. This classification of V1147 Tau is similar to that mentioned recently in the extended *Hipparcos* catalogue (Anderson & Francis 2012; Griffin 2012). We have also determined the bolometric luminosity ($L_{\rm bol}$) of V1147 Tau using the relations given in Landolt-Bornstein (Schmidt-Kaler 1982). The resulting values are given in Table 5. Using the improved colour temperature relation given by Houdashelt, Bell & Sweigart (2000), the effective temperature of V1147 Tau was estimated to be 4250 K. This value is consistent with that derived from SED.

We have computed the galactic space velocity components (U, V, W) and their associated errors of V1147 Tau using the procedure described by Johnson & Soderblom (1987). Parallax, proper motion and radial velocity, respectively, are taken from (Röser et al. 2011), (Perryman et al. 1997) and (Bobylev et al. 2006), which are given in Table 5. The values of (U, V, W) were calculated to be (−41.96 ± 0.56, −19.32 ± 0.48, −2.06 ± 0.31) km s^{-1}, respectively, which are close to the Hyades supercluster (−39.7, −17.7, −2.4). The total space velocity is computed to be $V_{\rm Total}$ = 46.24 ± 0.72. This star was found to be inside the boundaries for the young disc population in the (U, V) and (W, V) diagrams (Montes et al. 2001a). The (U, V, W) components of V1147 Tau indicate that it is a possible member of the 600 Myr Hyades supercluster (Montes et al. 2001b).

Lithium abundance is a well-known age indicator in late-type stars since this element is destroyed as the convective motions gradually mix the stellar envelope with hotter ($T \sim 2.5 \times 10^6$ K) inner

Table 5. Physical parameters of V1147 Tau.

Parameters	Values	Reference
Spectral type	K5V	Present study
V (mag)	11.07	Present study
$M_{\rm v}$ (mag)	7.70 ± 0.07	Present study
$M_{\rm bol}$ (mag)	6.93 ± 0.07	Present study
$T_{\rm eff}$ (K)	4250 ± 250	Present study
$\log g$	4.5 ± 0.5	Present study
$\log(\rm lx/L_{bol})$	-2.98	Present study
$L_*/L_\odot$	0.13 ± 0.02	Present study
$R_*/R_\odot$	0.67 ± 0.03	Present study
$M_*/M_\odot$ (primary)	0.79	Bender & Simon (2008)
$M_*/M_\odot$ (secondary)	0.58	Bender & Simon (2008)
Inclination (i)	$\sim 62^\circ$	Griffin (2012)
μ_α (mas yr^{-1})	103.37 ± 1.79	Perryman et al. (1997)
μ_δ (mas yr^{-1})	-19.91 ± 1.65	Perryman et al. (1997)
π (mas)	22.19 ± 0.71	Röser et al. (2011)
R_V	40.4 ± 0.6	Bobylev et al. (2006)

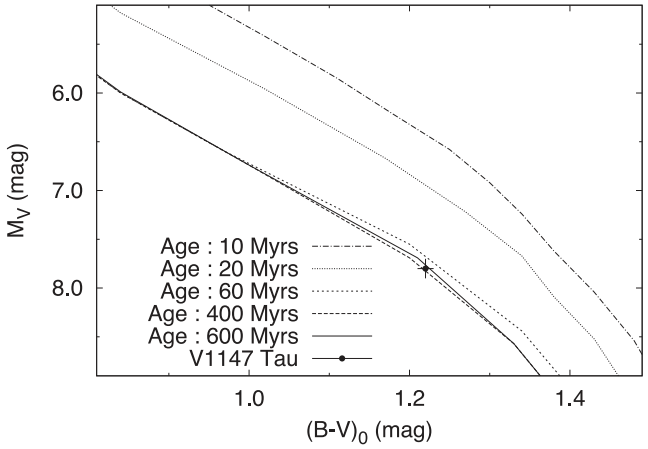

Figure 11. Colour–magnitude diagram of V1147 Tau with isochrones of 10, 20, 60, 400 and 600 Myr ages.

regions. For late K-, M-type stars, lithium is burned so rapidly that it is only detectable for extremely young stars (Maldonado et al. 2010). Barrado y Navascués & Stauffer (1996) have been measured the equivalent width of Li I ($\lambda = 6708$ Å) to be 10.7 ± 6 mÅ. We have compared this value with stars of similar spectral type (K5V with $B - V = 1.22$ and $V - I = 1.17$) in various moving group members of clusters (López-Santiago, Micela & Montes 2009; Maldonado et al. 2010). The EW(Li) and colours of V1147 Tau is located in between the Hyades and Pleiades moving groups. This indicates that V1147 Tau is young star with age of 120–600 Myr.

In order to further constrain the age of V1147 Tau, we have used pre-man-sequence isochrones from Siess, Dufour & Forestini (2000). Fig. 11 shows the colour–magnitude ($B - V$ versus M_V) for pre-main-sequence isochrones of the ages of 10, 20, 60, 400 and 600 Myr (from top to bottom). The position of V1147 Tau in the colour–magnitude diagram is in between 400 and 600 Myr isochrones, which is consistent to that of the age derived from kinematics and Li abundances.

9 DISCUSSION AND SUMMARY

Using ∼20 yr long-term V-band photometry we have obtained the rotational period of V1147 Tau to be 1.4845 ± 0.0001 d. The rotational period of V1147 Tau is similar to that of the orbital period 1.4846984 ± 0.0000003 d derived by Griffin (2012), indicating a synchronous system. Griffin (2012) also found the circular orbit of V1147 Tau. It is remarked that Glebocki & Stawikowski (1997) studying dwarf G–K binaries have found that the systems with orbital period less than about 10 d should rotate synchronously with their orbital revolution and their orbits should be circular. Most of RS CVn and BY Dra-type binaries are synchronized with the usually low eccentricities of their orbits. We have plotted eccentricity versus orbital period and orbital period versus rotational period in Figs 12(a) and (b), respectively, for 141 dwarf binaries taken from the catalogue of chromospherically active binaries due to Eker et al. (2008). The location of V1147 Tau is marked by open triangle. In Fig. 12(a), the limiting period marking the transition between circular and elliptical orbits is distinctive. The absence of points with $e < 0.10$ and $P > 10$ d is clearly apparent in Fig. 12. This means that binary systems are created with primarily elliptical orbits, and that circular orbits are produced by tidal evolution. Mermilliod & Mayor (1984) suggested that most of the orbital circularization could be determined by stellar evolution prior to arrival on the main sequence. Zahn & Bouchet (1989), who have extended it further, substantiate that most of the circularization occurs during the pre-main-sequence phase and predicted a value for the cut-off period of between 7 and 8.5 d. It also corresponds to the limit observed for field dwarfs in the solar neighbourhood (Duquennoy & Mayor 1991).

The variable shapes and amplitudes of light curves indicate the temperature inhomogeneities on the surface of V1147 Tau. The brightness variability amplitudes were found from 0.06 to 0.30 mag. The variability amplitude up to 0.4 mag were observed in similar type of stars (e.g. Alekseev 2000). A modelling of these observations reveals that the stellar surface of V1147 Tau is spotted up to 22 per cent, which is very similar to that found in K-type stars LQ Hya and MS Ser (Alekseev 2003). However, the spot coverage for the evolved RS CVn-type binaries were found up to 16 per cent (Padmakar & Pandey 1999). Most of the time spots were distributed along two longitudes. During the epochs 11–15 the light curves appear to be relatively flat with respect to the earlier epochs. This suggests that either the star now is dominated by peppered starspots over its surface (e.g. see Savanov & Strassmeier 2008), or it may be entering a Maunder minimum-like phase (Baliunas & Jastrow 1990; Baliunas et al. 1995). However, from the optical photometric light curves, it is difficult to attribute it to a minimum activity/Maunder minimum like state of a star as its level is below the so-called 'unspotted' brightness (or brightest state of the object). The Ca II H&K observations are important to see the Maunder minimum like activity (e.g. Lubin, Tytler & Kirkman 2012; Takeda et al. 2012).

In our light curve modelling we found the time of flip-flop coincides with the time of maximum surface spottedness. For the first time Savanov & Strassmeier (2008) noticed a coincidence of the flips and flops with the times of minimum light as well as minimum photometric amplitude for the star V1335 Ori. Indication of the flip-flop effect in V1147 Tau is quite similar to that observed by Korhonen et al. (2002) and Järvinen et al. (2005). The flip-flop phenomenon has been noticed for the first time by Jetsu et al. (1991) in the giant star FK Comae and also seen in many other active stars (e.g. Jetsu, Pelt & Tuominen 1993; Berdyugina & Tuominen 1998; Berdyugina et al. 2000). After its discovery in cool stars, the flip-flop phenomenon has also been reported in the Sun (Berdyugina & Usoskin 2003). This phenomenon is explained by the dynamo-based solution where a non-axisymmetric dynamo component, giving rise to two permanent active longitudes 180° apart, is needed

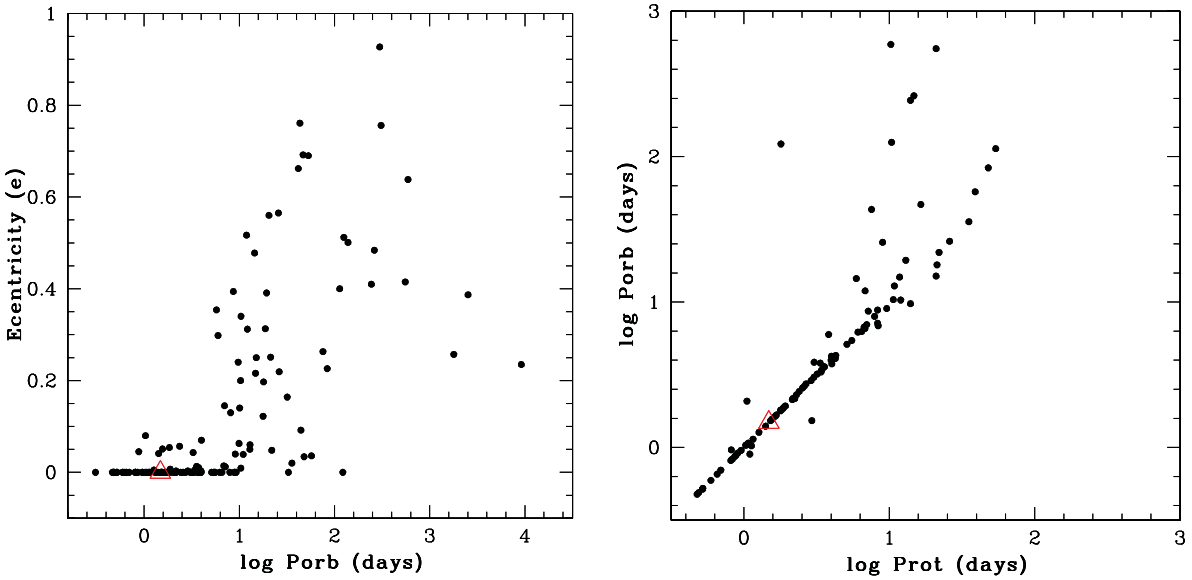

Figure 12. (a) Eccentricity as function of orbital period. (b) A plot of the rotational period versus orbital period for the Dwarf binaries. Location of V1147 Tau is denoted by open triangle.

together with an oscillating axisymmetric magnetic field (Elstner & Korhonen 2005; Korhonen & Elstner 2005). Fluri & Berdyugina (2004) suggest another possibility with a combination of stationary axisymmetric and varying non-axisymmetric components.

Polarimetric observations of V1147 Tau suggest the presence of a supplementary source of linear polarization, such as the remnant of the circumstellar disc. In several investigations, it has been suggested that the linear polarization in late-type dwarfs is closely related with magnetic activity and the consequent inhomogeneities on the stellar surface (e.g. Tinbergen & Zwaan 1981; Tinbergen 1982; Huovelin, Saar & Tuominen 1988). The polarization is believed to be sum of polarizations in saturated Zeeman sensitive absorption lines in the observed passband, via a phenomenon called the magnetic intensification (Leroy 1962; Calamai & Landi Degl'Innocenti 1975). Magnetic intensification in Zeeman sensitive absorption is suggested as the dominant effect connecting linear polarization with magnetic activity in the most active single late-type dwarfs, while the wavelength dependence in the less active stars could also be due to a combination of Rayleigh and Thomson scattering (Huovelin et al. 1989). The linear polarization may provide valuable information on the configuration of magnetic fields, if monitored simultaneously with other activity indicators (Saar et al. 1987; Huovelin et al. 1988).

We would like to compare and contrast our results with earlier similar investigations in the literature. The *ROSAT* X-ray observations of 35 BY Dra systems were studied by Dempsey et al. (1997), assuming that their coronae had solar abundances. The low-temperature component kT_1 and high-temperature component kT_2 for these systems were found in the ranges of (0.13–0.31) and (1.07–2.81) keV, respectively, which are similar to our results. However, kT_2 is found to be less than of that of BY Dra systems. Further, the average values of volume emission measures EM_1 and EM_2 for the BY Dra systems are $0.14 \pm 0.04 \times 10^{53}$ and $0.76 \pm 0.29 \times 10^{53}$ cm^{-3}, respectively. Compared to this, we obtain for V1147 Tau EM_1 to be 60–65 times more than the average value for BY Dra systems, whereas value of EM_2 is close to the average value the BY Dra systems. An analysis of the average and the median X-ray luminosity ($\log L_X$) for 101 dwarfs has been made by Pandey et al. (2005a) derived these parameters to be 29.6 ± 0.7 and 29.63 erg s^{-1}, respectively. We find that the inferred value of $\log L_X$ for V1147 Tau is close to the average value for active dwarf systems. The observed X-ray spectrum and the inferred coronal plasma parameters for V1147 Tau are typical of those seen in active stars such as BY Dra binaries.

The combined optical photometric, spectroscopic, polarimetric and X-ray data analyses indicate that V1147 Tau is highly active star of the class BY Dra at the age of about 0.4–0.6 Gyr. However, follow up X-ray as well as high-resolution optical spectroscopic observations are highly needed to probe the magnetic activities more deeply.

ACKNOWLEDGEMENTS

We feel highly obliged to the anonymous referee for his detailed constructive comments and valuable suggestions which led to significant improvements in the original manuscript. MKP and DCS acknowledge the financial support received from ISRO-RESPOND, India, under the project (ISRO/RES/2/362/09-10). VP acknowledges the financial support received from UGC, Govt of India under the fellowship (Fo. F. 142(SC)/2010 (SA)). MKP also acknowledges to ARIES for library and computational facilities. This research has made use of the data obtained from the High Energy Astrophysics Science Archive Research Center (HEASARC), provided by NASAs Godard Space Flight Center. STARLINK is funded by PPARC and based at the Rutherford Appleton Laboratory, which is part of the Council for the Central Laboratory of the Research Councils, UK.

REFERENCES

Agrawal P. C., Vaidya J., 1988, MNRAS, 235, 239
Alekseev I. Y., 2000, Astron. Rep., 44, 696
Alekseev I. Y., 2003, Astron. Rep., 47, 430
Alekseev I. Y., Kozlova O. V., 2003, A&A, 403, 205
Anders E., Grevesse N., 1989, Geochim. Cosmochim. Acta, 53, 197

Anderson E., Francis C., 2012, Astron. Lett., 38, 331
Arnaud K. A., 1996, in Jacoby G. H., Barnes J., eds, ASP Conf. Ser. Vol. 101, Astronomical Data Analysis Software and Systems. Astron. Soc. Pac., San Francisco, p. 17
Audard M., Behar E., Güdel M., Raassen A. J. J., Porquet D., Mewe R., Foley C. R., Bromage G. E., 2001, A&A, 365, L329
Bailer-Jones C. A. L., Mundt R., 2001, A&A, 367, 218
Baliunas S., Jastrow R., 1990, Nat, 348, 520
Baliunas S. L. et al., 1983, ApJ, 275, 752
Barrado y Navascués D., Stauffer J. R., 1996, A&A, 310, 879
Bender C. F., Simon M., 2008, ApJ, 689, 416
Berdyugina S. V., 2005, Living Rev. Sol. Phys., 2, 8
Berdyugina S. V., 2007, Highlights Astron., 14, 275
Berdyugina S. V., Tuominen I., 1998, A&A, 336, L25
Berdyugina S. V., Usoskin I. G., 2003, A&A, 405, 1121
Berdyugina S. V., Berdyugin A. V., Ilyin I., Tuominen I., 1998, A&A, 340, 437
Berdyugina S. V., Berdyugin A. V., Ilyin I., Tuominen I., 2000, A&A, 360, 272
Berdyugina S. V., Pelt J., Tuominen I., 2002, A&A, 394, 505
Bobylev V. V., Bajkova A. T., Gontcharov G. A., 2006, Astron. Astrophys. Trans., 25, 143
Bopp B. W., 1987, ApJ, 317, 781
Bopp B. W., Noah P. V., Klimke A., Africano J., 1981, ApJ, 249, 210
Brandenburg A., Dobler W., 2002, Astron. Nachr., 323, 411
Calamai G., Landi Degl'Innocenti E., 1975, A&A, 45, 297
Catalano S., Frasca A., 1994, A&A, 287, 575
Catalano S., Rodono M., Frasca A., Cutisspoto C., 1996, in Strassmeier K. G., Linsky J. L., eds, Proc. IAU Symp. 176, Stellar Surface Structure. Kluwer Academic Publishers, Dordrecht, p. 403
Cieza L. A., William D. C., Jean-Charles A., 2008, ApJ, 679, 720
Collier Cameron A., 1992, in Byrne P. B., Mullan D. J., eds, Lecture Notes in Physics, Vol. 397, Surface Inhomogeneities on Late-Type Stars. Springer-Verlag, Berlin, p. 33
Cutri R. M. et al., 2003, VizieR Online Data Catalog, II/246
Cutri R. M. et al., 2012, VizieR Online Data Catalog II/311/wise
Delorme P., Collier Cameron A., Hebb L., Rostron J., Lister T. A., Norton A. J., Pollacco D., West R. J., 2011, MNRAS, 413, 2218
Dempsey R. C., Linsky J. L., Fleming T. A., Schmitt J. H. M. M., 1997, ApJ, 478, 358
Deutsch A. J., 1958, in Lehneart B., ed., Proc. IAU Symp. 6, Electromagnetic Phenomena in Cosmical Physics, Cambridge Univ. Press, Cambridge, p. 209
Dhillon V. S., Privett G. J., Duffey K. P., 2001, PERIOD – A Time-Series Analysis Package, version 5.0 (http://www.starlink.rl.ac.uk/star/docs/sun167.htx/sun167.html)
Dobler W., Stix M., Brandenburg A., 2006, ApJ, 638, 336
Donati J.-F., Forveille T., Collier Cameron A., Barnes J. R., Delfosse X., Jardine M. M., Valenti J. A., 2006, Sci, 311, 633
Duquennoy A., Mayor M., 1991, A&A, 248, 485
Durney B. R., Robinson R. D., 1982, ApJ, 253, 290
Eker Z. et al., 2008, MNRAS, 389, 1722
Elias N. M., II, Dorren J. D., 1990, AJ, 100, 818
Elstner D., Korhonen H., 2005, Astron. Nachr., 326, 278
Elvis E., Plummer D., Schachter J., Fabbiano G., 1992, ApJS, 80, 257
Fluri D. M., Berdyugina S. V., 2004, Sol. Phys., 224, 153
Gálvez M. C., Montes D., Fernandez-Figueroa M. J., Lopez-Santiago J., De Castro E., Cornide M., 2002, A&A, 389, 524
Gilman P. A., 1983, ApJS, 53, 243
Glebocki R., Stawikowski A., 1997, A&A, 328, 579
Golovin A. et al., 2012, MNRAS, 421, 132
Goncharskii A. V., Stepanov V. V., Kokhlova V. L., Yagola A. G., 1977, Sov. Astron. Lett., 3, 147
Griffin R. F., 2012, JA&A, 33, 29
Güdel M., Guinan E. F., Skinner S. L., 1997, ApJ, 483, 947
Houdashelt M. L., Bell R. A., Sweigart A. V., 2000, AJ, 119, 1448
Huovelin J., Saar S. H., 1991, ApJ, 374, 319
Huovelin J., Saar S. H., Tuominen I., 1988, ApJ, 329, 882
Huovelin J., Linnaluoto S., Tuominen I., Virtanen H., 1989, A&AS, 78, 129
Järvinen S. P., Berdyugina S. V., Tuominen I., Cutispoto G., Bos M., 2005, A&A, 432, 657
Jetsu L., Pelt J., Tuominen I., Nations H., 1991, in Tuominen I., Moss D., Rdiger G., eds, Proc. IAU Colloq. 130, The Sun and Cool Stars: Activity, Magnetism, Dynamos. Springer-Verlag, Berlin, p. 381
Jetsu L., Pelt J., Tuominen I., 1993, A&A, 278, 449
Johnson D. R. H., Soderblom D. R., 1987, AJ, 93, 864
Kazarovets E. V., Samus N. N., Durlevich O. V., Frolov M. S., Antipin S. V., Kireeva N. N., Pastukhova E. N., 1999, Inf. Bull. Var. Stars, 4659, 1
Kitchatinov L. L., Rüdiger G., 1999, A&A, 344, 911
Kopal Z., 1968, Ap&SS, 1, 411
Korhonen H., Elstner D., 2005, A&A, 440, 1161
Korhonen H., Berdyugina S. V., Tuominen I., 2002, A&A, 390, 179
Kürster M., 1993, A&A, 274, 851
Kürster M., Schmitt J. H. M. M., Cutispoto G., Dennerl K., 1997, A&A, 320, 831
Kurucz R. L., 2000, Available at: http://www.cfaku5.harvard.edu
Lanza A. F., Catalano S., Cutispoto G., Pagano I., Rodonó M., 1998, A&A, 332, 541
Leroy J. L., 1962, Ann. Astrophys., 25, 127
López-Santiago J., Micela G., Montes D., 2009, A&A, 499, 129
Lubin D., Tytler D., Kirkman D., 2012, ApJ, 747, L32
Maldonado J., Martínez-Arnáiz R. M., Eiroa C., Montes D., Montesinos B., 2010, A&A, 521, A12
Medhi B. J., Maheswar G., Brijesh K., Pandey J. C., Kumar T. S., Sagar R., 2007, MNRAS, 378, 881
Medhi B. J., Maheswar G., Pandey J. C., Kumar T. S., Sagar R., 2008, MNRAS, 388, 105
Mermilliod J. C., Mayor M., 1984, in Maeder A., Renzini A., eds, Proc. IAU Symp. 105, Observational Tests of the Stellar Evolution Theory. Kluwer, Dordrecht, p. 411
Mohanty S., Basri G., 2003, ApJ, 583, 451
Montes D., Fernández-Figueroa M. J., de Castro E., Cornide M., Latorre A., 2001a, in Garcia Lopez J., Rebolo R., Zapaterio M. R., eds, ASP Conf. Ser. Vol. 223, 11th Cambridge Workshop on Cool Stars, Stellar Systems and the Sun. Astron. Soc. Pac., San Francisco, p. 1477
Montes D., López-Santiago J., Gálvez M. C., Fernández-Figueroa M. J., De Castro E., Cornide M., 2001b, MNRAS, 328, 45
Mullis C. L., Bopp B. W., 1994, PASP, 106, 822
Noyes R. W., Hartmann L. W., Baliunas S. L., Duncan D. K., Vaughan A. H., 1984, ApJ, 279, 763
Oláh K., Kövari Zs., Bartus J., Strassmeier K. G., Hall D. S., Henry G. W., 1997, A&A, 321, 811
Padmakar P. S., Pandey S. K., 1999, A&AS, 138, 203
Pandey J. C., Singh K. P., 2008, MNRAS, 387, 1627
Pandey J. C., Singh K. P., 2012, MNRAS, 419, 1219
Pandey J. C., Singh K. P., Drake S. A., Sagar R., 2005a, AJ, 103, 1231
Pandey J. C., Singh K. P., Drake S. A., Sagar R., 2005b, JA&A, 26, 359
Pandey J. C., Medhi Biman J., Sagar R., Pandey A. K., 2009, MNRAS, 396, 1004
Perryman M. A. et al., 1997, A&A, 323, L49
Pfeffermann E. et al., 1987, Proc. SPIE, 733, 519
Piskunov N. E., Kochukhov O., 2002, A&A, 381, 736
Pojmaski G., 2002, Acta Astron., 52, 397
Prabhu T. P., Anupama G. C., Surendiranath R., 1998, Bull. Astron. Soc. India, 26, 383
Rautela B. S., Joshi G. C., Pandey J. C., 2004, Bull. Astron. Soc. India, 32, 159
Rice J. B., Wehlau W. H., Khokhlova V. L., 1989, A&A, 208, 179
Roberts D. H., Lehar J., Dreher J. W., 1987, AJ, 93, 968
Röser S., Schilbach E., Piskunov A. E., Kharchenko N. V., Scholz R.-D., 2011, A&A, 531, 92
Rostopchina A. N., Grinin V. P., Shakhovskoi D. N., Lomach A. A., Minikulov N. Kh., 2007, Astron. Rep., 51, 55
Saar S. H., Huovelin J., 1993, ApJ, 404, 739

Saar S. H., Huovelin J., Giampapa M. S., Linsky J. L., Jordan C., 1987, in Havnes O., Pettersen B. R., Schmitt J., Solheim J. E., eds, Activity in Cool Envelopes. Kluwer, Dordrecht, p. 45
Savanov I. S., 2009, Astron. Rep., 53, 941
Savanov I. S., 2010, Astron. Rep., 54, 437
Savanov I. S., Dmitrienko E. S., 2011, Astron. Rep., 55, 437
Savanov I. S., Strassmeier K. G., 2005, A&A, 444, 931
Savanov I. S., Strassmeier K. G., 2008, Astron. Nachr., 329, 364
Scalitriti F., Piirola V., Coyne G. V., Koch R. H., Elias N. M., Holenstein B. D., 1993, A&AS, 102, 343
Schachter J. F., Remillard R., Saar S. H., Favata F., Sciortino S., Barbera M., 1996, ApJ, 463, 747
Schmidt G. D., Elston R., Lupie O. L., 1992, AJ, 104, 1563
Schmidt-Kaler Th., 1982, in Scaifers K., Voigt H. H., eds, Landolt-Bornstein: Numerical Data and Functional Relationship in Science and Technology, New series, Group VI, Vol. 2b. Springer-Verlag, Berlin
Siess L., Dufour E., Forestini M., 2000, A&A, 358, 593
Skumanich A., 1972, ApJ, 171, 565
Smith R. K., Brickhouse N. S., Liedahl D. A., Raymond J. C., 2001, ApJ, 556, L91
Stauffer J. R., Balachandran S. C., Krishnamurthi A., Pinsonneault M., Terndrup D. M., Stern R. A., 1997, ApJ, 475, 604
Stelzer B., Neuhaeuser R., Hambaryan V., 2000, A&A, 356, 949
Strassmeier K. G. et al., 1991, A&A, 247, 130
Strassmeier K. G. et al., 2008, A&A, 490, 287
Takeda Y., Tajitsu A., Honda S., Kawanomoto S., Ando H., Sakurai T., 2012, PASJ, 64, 130
Tas G., Evren S., Ibanoğ C., 1999, A&A, 349, 546
Tinbergen J., 1982, A&A, 105, 53
Tinbergen J., Zwaan C., 1981, A&A, 101, 223
Torres G., Andersen J., Giménez A., 2010, A&AR, 18, 67
Trümper R. A., 1983, Adv. Space Res., 2, 241
Unruh Y. C., Collier Cameron A., 1995, MNRAS, 290, 37
Voges W. et al., 1999, A&A, 349, 389
Vogt S. S., 1981, ApJ, 250, 327
Vogt S. S., Penrod G. D., 1983, PASP, 95, 565
Yudin R. V., Evans A., 2002, A&A, 386, 916
Zahn J. P., 1977, A&A, 57, 394
Zahn J. P., Bouchet L., 1989, A&A, 223, 112

This paper has been typeset from a TEX/LATEX file prepared by the author.